REVIEWS SCIENCE CHINA Materials

mater.scichina.com link.springer.com

Published online 23 January 2015 | doi: 10.1007/s40843-015-0017-6
Sci China Mater 2015, 58: 60–76

ZnO nanostructures in enzyme biosensors

Yue Zhang[1,2*], Zhuo Kang[1], Xiaoqin Yan[1] and Qingliang Liao[1]

Biosensing has developed tremendously since it was demonstrated by Leland C. Clark Jr. in 1962. ZnO nanomaterials are attractive candidates for fabricating biosensors, because of their diverse range of nanostructures, high electron mobility, chemical stability, electrochemical activity, high isoelectric points which promote enzyme adsorption, biocompatibility, and piezoelectric properties. This review covers ZnO nanostructures applied in enzyme biosensors, in the light of electrochemical transduction and field effect transduction. Different assembly processes and immobilization methods have been used to load enzymes into various ZnO nanostructures, providing enzymes with favorable micro-environments and enhancing their sensing performance. We briefly describe recent trends in ZnO syntheses, and the analytical performance of the fabricated biosensors, summarize the advantages of using ZnO nanostructures in biosensors, and conclude with future challenges and prospects.

INTRODUCTION

A biosensor is an analytical device consisting of a biomatrix (e.g., enzymes, antibodies, nucleic acids, receptors, organelles, microorganisms) and transducer (e.g., electrochemical, photometric, acoustic/mechanical, piezoelectric, calorimetric), which converts biological information into measurable signals [1–3]. Enzyme biosensors in particular have attracted much attention [4]. Enzymes are sensing elements with specificity and catalytic properties. They have been widely integrated with transducers by various immobilization techniques (e.g., physical adsorption, cross-linking, covalent linkage, embedding, encapsulation, entrapment) to construct biosensors. Such biosensors have been applied in medical diagnostics, health care, food industries, agriculture, military and defense industries, environmental monitoring and biotechnology [5]. Fig. 1 shows the fundamental working principles of an enzyme biosensor.

Characterization techniques have been improved, and new synthesis methods have been developed in recent years. This has led to a focus on enhancing biosensor performance by incorporating nanomaterials, and ZnO has been an attractive candidate. Its diverse range of nanostructures includes particles, wires, rods, needles, belts, tubes, fibers, tetrapod-like, flower-like and hedgehog-like morphologies. ZnO possesses significant sensing surface, chemical stability, a wide direct band gap (3.37 eV), large excitation binding energy (60 meV), high refractive index (2.0041), high electron mobility (210 $cm^2\ V^{-1}\ s^{-1}$), low toxicity, and piezoelectric and ultraviolet protection properties. ZnO is biocompatible [6,7] and has a high isoelectric point (IEP) of ~9.5, which is suitable for electrostatically adsorbing proteins with low IEPs [8–10]. ZnO is relatively stable at physiological pH, compatible with biological fluids and species [6], and therefore suitable for *in vivo* application. While the redox capabilities of enzymes are not typically enhanced because of their insulated redox centers, specific ZnO nanostructures can facilitate direct electron transfer (DET) between enzyme electroactive sites and external electrodes [9,11–14]. The synthesis of ZnO nanostructures by different techniques has promoted the fabrication of enzyme biosensors.

In the following sections we review the state-of-the-art ZnO nanostructure-based enzyme biosensors, including ZnO syntheses, and biosensor construction and performance. We discuss how the development of nanotechnology may promote sensing, and highlight the essential characteristics of ZnO nanostructure-based enzyme biosensors, to allow for advancement of biosensing techniques.

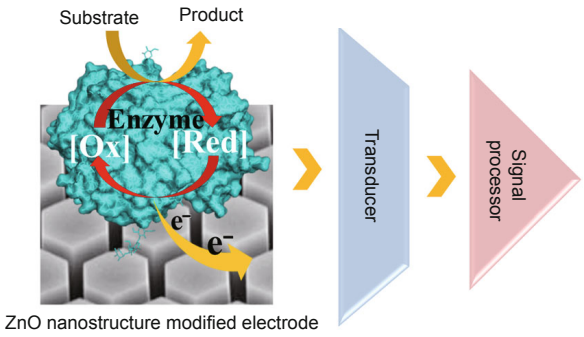

Figure 1 Working principles of a ZnO nanostructure-based enzyme biosensor.

[1] State Key Laboratory for Advanced Metals and Materials, School of Materials Science and Engineering, University of Science and Technology Beijing, Beijing 100083, China
[2] Key Laboratory of New Energy Materials and Technologies, University of Science and Technology Beijing, Beijing 100083, China
* Corresponding author (email: yuezhang@ustb.edu.cn)

BIOSENSORS BASED ON ELECTROCHEMICAL TRANSDUCTION

Electrochemical biosensors are the most common biosensors, and are more efficient than conventional measurement techniques such as NMR spectroscopy [15], radioisotope tracing [16–19] and microfluorometric assays [20,21]. This is because of their comparable instrument sensitivity, high range of detection, real-time monitoring capability, ease of fabrication and control, reproducibility and low cost. Amperometry, potentiometry, cyclic voltammetry (CV), differential pulse voltammetry (DPV) and electrochemical impedance spectroscopy (EIS) are the most common electrochemical techniques used in biosensors [22]. Much recent attention has been focused on amperometric measurements, because they can yield a linear relationship between sensor output and analyte concentration. Potentiometric measurements usually lack high sensitivity, because of the semi-logarithmic relationship between sensor output and analyte concentration [23].

Detection of glucose

Glucose is important in many biochemical pathways, such as glycolysis. A high glucose level in human blood is indicative of diabetes mellitus, a metabolic disorder resulting from defective pancreatic function. The importance of measuring glucose levels, and the fact that glucose is commonly oxidized by enzymes, has led to most biosensors focusing on glucose. Glucose biosensors are based on the recognition of glucose by the enzyme glucose oxidase (GOx), which converts glucose and O_2 into gluconic acid and hydrogen peroxide (H_2O_2). H_2O_2 is then electrochemically oxidized at +500 mV *vs*. Ag/AgCl.

$$\text{Glucose} + O_2 \rightarrow \text{Gluconic acid} + H_2O_2, \quad (1)$$

$$H_2O_2 \rightarrow O_2 + 2H^+ + 2e^-. \quad (2)$$

The morphology of the nanostructure significantly affects its electrochemical properties, so numerous ZnO nanostructures have been investigated for application in glucose biosensors. The following discussion progresses from simple nanostructures to complex nanohybrids, to illustrate the influence of ZnO nanostructure on the glucose biosensor performance.

Simple ZnO nanostructures for GOx immobilization

Nanostructure matrices provide a solid support for immobilizing sensing molecules. The physical, chemical and surface properties of the desired support determine the method of enzyme immobilization, the nature of the immobilized sensing molecules, and the overall biosensor performance [24]. ZnO matrices are superior to their TiO_2 analogues, with respect to the adsorption and bioelectrochemistry of proteins [25]. The high surface-to-volume ratio of ZnO nanostructures provides a large specific surface area for the adsorption of GOx, and thus comparatively more active sites for catalysis.

In the traditional method, ZnO nanostructures are transferred to the surface of a working electrode to form a thin layer as the modification on transducers. ZnO nanotetrapods possessing four single crystalline legs were synthesized by vapor-phase transport (Fig. 2a) [26]. The nanotetrapods were transferred onto a standard Au electrode, to form a multiterminal network GOx adsorption layer. The three-dimensional (3D) structure based on ZnO nanotetrapods enhanced the sensitivity for glucose (25.3 $\mu A\ mM^{-1}\ cm^{-2}$), resulting in a detection limit of 4 μM. The linear response range was 0.005–6.5 mM, and the response was stable. The result was attributed to the one-dimensional (1D) structure of individual nanotetrapods, their 3D stacked network, and their multiterminal electron communication capability. A carbon paste electrode modified with ZnO nanoparticles (NPs) of diameter <100 nm was applied in a biosensor [27], which exhibited a linear response range of 9.1×10^{-3}–14.5×10^{-3} mM, with high selectivity and reproducibility. The apparent Michaelis-Menten constant (K_M^{app}) and maximum reaction current response (I_{max}) were 0.124 mM and 2.033 μA, respectively. This indicated that the ZnO NP-modified carbon paste maintained the activity of GOx, and provided suitable pathways for electron transfer between GOx and the electrode. The determination of glucose in human serum demonstrated the practical application of the ZnO NP-modified carbon paste, at a 95% confidence level. ZnO nanocombs (Fig. 2b) were also synthesized by vapor phase transport [9], and their structure was investigated by scanning electron microscopy (SEM), transmission electron microscopy (TEM) and selected area electron diffraction. The ZnO nanocombs were used as the support material in a biosensor, which exhibited a sensitivity of 15.33 $\mu A\ mM^{-1}\ cm^{-2}$ without the presence of an electron mediator, and a K_M^{app} of 2.19 mM. The single crystalline ZnO nanocombs provided many electron transfer channels, which enhanced sensor performance. Ahmad *et al.* [28] prepared ZnO nanofibers with diameters of 195–350 nm through electrospinning, which is widely used to produce polymer fibers. A single nanofiber was transferred to a Au electrode, and functionalized with GOx to yield a glucose biosensor. Exposure to ultraviolet light for 2 h increased the current response of the ZnO NP-based glucose biosensor by ~30%, and the detection limit decreased by two orders of magnitude, compared with the response in the absence of light [29]. However, the mechanism of the enhanced photoelectrochemical response was not clearly elucidated.

In contrast from transferring ZnO nanostructures to an electrode surface, nanostructures have also been di-

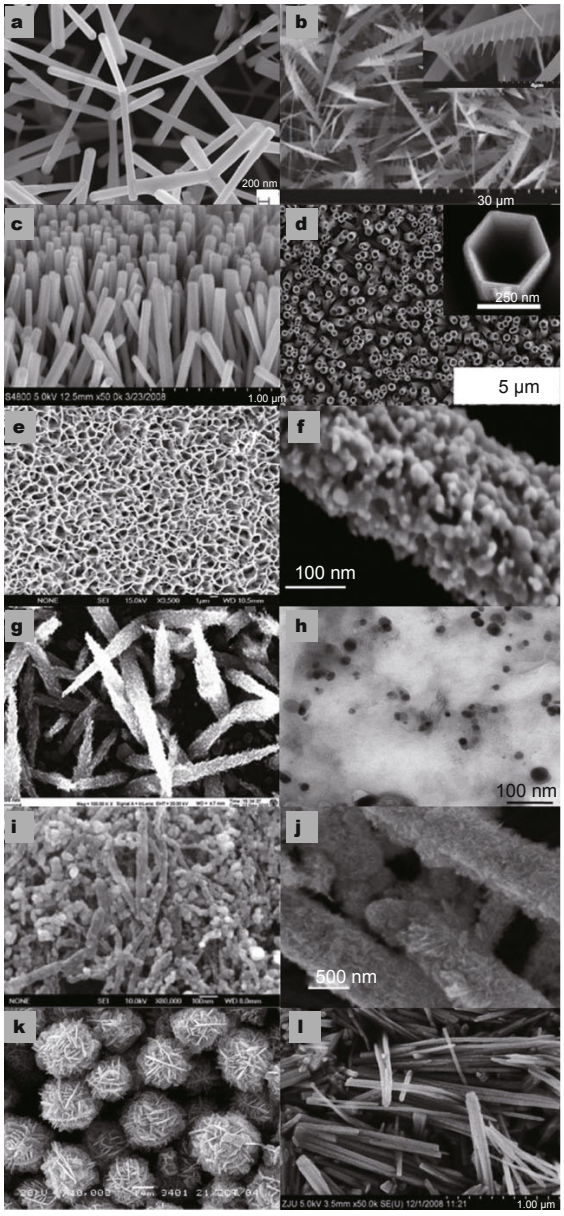

Figure 2 Morphologies of ZnO nanostructures: (a) SEM image of ZnO nanotetrapods; (b) SEM image of ZnO nanocombs, inset: high magnification; (c) SEM cross-sectional view of aligned ZnO nanorods; (d) SEM image of ZnO nanotube array; (e) SEM image of nanoflake ZnO; (f) SEM image of a ZnO nanofiber, showing pores and protuberances; (g) SEM image of prickly ZnO/Cu; (h) TEM image of ZnO NP-coated graphene; (i) SEM image of ZnO NPs grown on MWCNTs; (j) SEM image of ZnO micro-tubes; (k) SEM image of flower-like ZnO; (l) SEM image of fork-like ZnO nanostructures. Reproduced with permission from: (a) Ref. [26], Copyright 2010, Elsevier; (b) Ref. [9], Copyright 2006, AIP Publishing LLC; (c) Ref. [31], Copyright 2009, Elsevier; (d) Ref. [37], Copyright 2009, American Chemical Society; (e) Ref. [40], Copyright 2010, Elsevier; (f) Ref. [47], Copyright 2013, Elsevier; (g) Ref. [48], Copyright 2012, American Chemical Society; (h) Ref. [13], Copyright 2012, Elsevier; (i) Ref. [49], Copyright 2011, Elsevier; (j) Ref. [50], Copyright 2013, Royal Society of Chemistry; (k) Ref. [51], Copyright 2005, Elsevier; (l) Ref. [52], Copyright 2010, Elsevier.

rectly grown on transducers (Fig. 2c). ZnO nanorods were directly grown via hydrothermal decomposition on a Au electrode [30]. In phosphate buffered solution at pH 7.4, negatively-charged GOx was electrostatically immobilized on positively charged ZnO. The resulting sensor exhibited a linear response in the range of 0.01–3.45 mM, and a sensitivity of 23.1 μA mM^{-1} cm^{-2}. A Nafion membrane layer was then introduced outside the ZnO nanorod film, and the resulting biosensor exhibited excellent selectivity against uric and ascorbic acids. This demonstrated the protection properties of Nafion, which can suppress anionic interference [31]. The aspect ratio (AR) of the well-aligned ZnO nanorods grown directly on a Si/Ag electrode was controlled to optimize the performance of the resulting biosensor [32]. The biosensor with an AR of 60 exhibited a sensitivity of 110.76 μA mM^{-1} cm^{-2}, a K_M^{app} of 0.137 mM, and a response time of < 1 s. This demonstrated that the ZnO nanorod array with high specific surface area provided a favorable microenvironment for immobilized GOx, and efficient electroconducting tunnels for electron transfer. Kim *et al.* [33] improved the performance of glucose sensors, by tailoring the surface area of ZnO nanorod array. Aligned ZnO nanorods grown directly on the electrode exhibited better performance than randomly distributed nanorods. This was attributed to the aligned single crystal nanorods facilitating faster heterogeneous electron transfer, and electrons only having to travel down a single rod, rather than jumping between rods before transferring into the electrode. Pradhan *et al.* [34] deposited a ZnO nanorod array on a Au-coated polyester substrate, to form a flexible enzymatic glucose biosensor. This illustrated the feasibility of realizing light-weight, flexible, high-performance sensing devices using ZnO nanostructures.

The influence of the two above-described assembly processes on biosensing performance was directly compared by Lei *et al.* [35], who constructed biosensors based on transferred and directly grown ZnO nanorods. That based on the ZnO nanorod array directly grown on a Au electrode exhibited better performance than that based on a transferred ZnO nanorod powder. This was consistent with the above-described experiments, and demonstrated the importance of good electrical contact between the nanomaterial and electrode. Another important contact exists between the enzyme and the nanomaterial, which can also significantly affect biosensor performance. The effect of the coupling agents, (3-aminopropyl) trimethoxysilane, (3-aminopropyl) triethoxysilane, and (3-aminopropyl) methyldiethoxysilane (APS), on the covalent immobilization of GOx on ZnO nanorods was studied [36]. The APS-treated glucose sensor exhibited the highest sensitivity and lowest K_M^{app}, which was attributed to the APS-treated ZnO nanowires containing the largest number of C–N

groups, and thus the lowest electron transfer resistance.

Immobilizing GOx on more complex ZnO nanostructures as working electrodes to detect glucose has also been investigated [12,37–43]. Yang *et al.* [37] prepared a highly oriented single-crystal ZnO nanotube array (Fig. 2d) through a two-step electrochemical/chemical process, on indium-doped tin oxide (ITO)-coated glass in aqueous solution. The sensitivity and linear calibration range of the biosensor were 30.85 μA mM^{-1} cm^{-2} and 10 μM–4.2 mM, respectively. A similar ZnO nanostructure was synthesized by chemically etching ZnO nanorods, electrochemically deposited on a Au surface [38]. GOx was then immobilized by cross-linking. The resulting biosensor exhibited a sensitivity, linear range, and detection limit of 21.7 μA mM^{-1} cm^{-2}, 50 μM–12 mM, and 1 μM, respectively. Both biosensors exhibited a wider linear range than the ZnO nanorod-based biosensors. The superior performance of the ZnO nanotubes was attributed to their porous structure, which provided a higher surface area than the flat nanorods. The 3D structure may also have prevented GOx from aggregating, and allowed H_2O_2 to rapidly diffuse to the electrode for oxidation. Tetragonal pyramid-shaped porous ZnO nanostructures were synthesized, and their high surface area and good compatibility with enzyme molecules were exploited for GOx immobilization [12]. The high efficiency of the nanostructure as an enzyme matrix was evident from its electron transfer rate constant (k_s) of 7.5 s^{-1}, during the direct electrochemical process. The formal potential of −0.464 V is comparable to the standard electrode potential of −0.46 V (*vs*. the saturated calomel electrode), for flavin adenine dinucleotide (FAD)/$FADH_2$ at pH 7.0. For a practical serum sample, the biosensors exhibited good accuracy and practicability, with recoveries of 95%–103%. A potentiometric intracellular glucose biosensor was fabricated, by immobilizing GOx on nanoflake ZnO grown on the tip of a borosilicate glass capillary [40]. The nanoflake ZnO (Fig. 2e) had a wall thickness of ~200 nm, and formed a honeycomb structure. The structure provided a large surface area to offset the small capillary tip, and led to a high capture efficiency. The potential difference of the biosensor showed linear dependence with the logarithem of the glucose concentration from 500 nM to 10 mM, and the response time was ⩽ 4 s. Intracellular glucose measurements in human adipocytes and frog oocytes were consistent with the previously reported values. The monitoring capability of the sensor was demonstrated by the increased intracellular glucose concentration induced by insulin treatment. Overall, nanoflake ZnO is promising for the reliable measurement of intracellular glucose concentrations in living cells. A similar intracellular biosensor based on hexagonal ZnO nanorods grown on the tip of a Ag-covered borosilicate glass capillary was also reported [41].

Biological systems can provide an ideal environment for synthesizing nanomaterials with controlled morphologies and crystal structures [44–46]. Nanostructures replicated from biological templates can combine the merits of the material itself and the biological structure. Biomorphic porous ZnO nanostructures were synthesized through an aqueous sol-gel soaking process, using pieces of apple flesh and skin as templates. The resulting nanostructures were exploited in glucose direct electrochemical biosensors [42]. The nanostructure prepared using the apple skin template better facilitated the electron transfer of immobilized GOx, than that prepared using the apple flesh. This may be because of the differing morphology and smaller average crystallite size of the former nanostructure. Silk was proposed as a biotemplate for fabricating mesoporous multiwalled ZnO nanotubes for glucose biosensing [43]. The prepared nanostructure possessed a size-adaptive mesoporous micro environment for enzyme loading, and excellent water permeability for analyte diffusion. The biosensor had a response time of ⩽ 2 s, which was attributed to the fast diffusion of reactants, and 1D channels facilitating electron transfer.

ZnO-based nanocomposites for GOx immobilization

Nanocomposites of ZnO (and other nanomaterials) including metal oxide semiconductor-metal hybrids and inorganic-organic hybrids [53], have also been used as matrices for enzyme immobilization. The hybridization of individual nanostructures can combine or even improve the properties of each component.

An organic-inorganic hybrid of mesoporous ZnO/chitosan with a single 1D nanostructure (Fig. 2f), was used to fabricate a probe-type glucose biosensor. This demonstrated the feasibility of using a single 1D nanostructure as a nanoprobe for biosensing in single cells or microorganisms [47]. A core-shell nanocomposite based on ZnO encapsulated by chitosan-graft-poly (vinyl alcohol) (PVA) was used to fabricate a potentiometrically-tuned glucose biosensor [54]. It exhibited fast surface-controlled redox biochemistry, with a detection limit of 0.2 μM, a linear range of 2 μM–1.2 mM, and a sensitivity of > 0.04 V $μM^{-1}$. The latter was attributed to the catalytic nature of the ZnO NPs, and the favorable adsorption of GOx by the biocompatible nanocomposite. The organic outer layer provided a compatible microenvironment for GOx, which promoted the performance of the biosensor.

Metal NPs are typically characterized by their high surface activity, large specific surface area, good electron conductivity, strong biomolecule adsorbability and biocompatibility [55–57]. Wei *et al.* [58] grew Au nanocrystals on the surface of ZnO nanorods, via a facial hydrothermal route. The resulting composite was used as a matrix to entrap

GOx via cross-linking. The resulting biosensor exhibited a linear response to glucose over the concentration range of 0.1–33.0 μM, and a detection limit and sensitivity of 10 nM and 1, 492 μA mM^{-1} cm^{-2}, respectively. In a Au-coated ZnO nanorod array-based biosensor [59], the ZnO/Au interface acted as a Schottky barrier, blocking electron transfer from ZnO to the enzyme. This increased the electron density at the ZnO conduction band, and improved the efficiency of the glucose sensor. ZnO nanorods were functionalized with a Au/Pt hybrid, in a multi-step chemosynthesis [60]. The resulting nanocomposite was used as an amperometric glucose biosensor. The high electrocatalytic activity of the composite resulted in the biosensors linear range of 1.8 μM–5.15 mM and detection limit of 0.6 μM. Huh *et al.* [61] modified a periodic hybrid Au/ZnO array, for use as an electrochemical glucose biosensor. The nanostructure was created by heat treating a spin-coated zinc acetate-PVA-Au layer on a surface relief grating, without requiring complex or expensive processing. Prickly ZnO/Cu nanocomposites (Fig. 2g) were grown directly on electrode substrates via the corrosion method [48]. The resulting composite had a large specific surface area, and led to improved electrical contact and sensing, thus providing a good platform for direct electrochemical reaction by the enzyme. In such decorated nanocomposites, the ZnO nanostructures serve as nucleation sites for metal nanomaterial growth at surface defects, and as electrical contacts to the metal NPs for integration into devices.

Doped ZnO nanostructures have been investigated for use in glucose biosensors. NiO-doped ZnO nanorods were hydrothermally prepared, and exploited in an amperometric glucose biosensor [62]. The biosensor exhibited a maximum electrochemical performance when the doping concentration was 7%. The NiO-doped ZnO nanorods had a high effective surface area, and thus a high number of active sites that favored GOx adsorption. The sensor exhibited a sensitivity of 61.78 μA mM^{-1} cm^{-2}. Porous ZnO: Co nanoclusters with an average particle size of 5 nm were synthesized by nanocluster-beam deposition. They were incorporated into a glucose sensor via Nafion-assisted cross-linking [63]. The ZnO: Co nanostructure had a high number of active sites, and high electrocatalytic activity.

Interest in carbon nanomaterials has increased tremendously in recent years, with graphene and carbon nanotubes (CNTs) having received much attention [64,65]. ZnO nanocomposites containing these nanomaterials have also been applied in biosensors [11,13,14,66–76]. Graphene/ZnO NPs hybrids (Fig. 2h) were used in a glucose biosensor with DET capability [13]. Zinc benzoate dihydrazinate was used as a single source precursor, to generate ZnO NPs which uniformly decorated graphene nanosheets at 200°C. The resulting nanohybrids exhibited antibacterial activity against *E.coli*, a gram negative bacteria, suggesting their potential in biosensing and bioengineering. ZnO NPs [14,72,73], ZnO micro-sponges [74], ZnO micro-flowers [75], and ZnO trigonal/tetragonal pyramids [76] were electrochemically deposited on multiwalled carbon nanotubes (MWCNTs) [14,72–74] and reduced graphene oxide [75,76], respectively. The resulting biosensors exhibited good electrocatalytic activity with fast electron transfer towards glucose. ZnO NPs were incorporated on MWCNTs by a microwave-assisted hydrothermal method, to realize the direct electrochemistry of GOx [14]. A similar report based on the same structure demonstrated a sensitive and stable glucose biosensor. This was attributed to the synergistic effect of the negatively-charged MWCNTs and positively charged ZnO NPs, and a polydiallyldimethylammonium chloride layer to suppress GOx leakage [72]. Besides, anti-interference capability to common chemicals was acquired by applying a lower working potential. This was attributed to the high electrocatalytic activity towards H_2O_2, through the adoption of ZnO/MWCNTs. While introducing MWCNTs promoted the electrocatalytic properties of these biosensors, the biosensor mechanism was unclear. Most MWCNT reagents contain metal impurities derived from catalysts used during growth, which likely contribute to the observed electrochemical activity. Such interference complicates the understanding of the electrochemical mechanism, but demonstrates that electrochemical performance can be promoted by introducing catalytic metal NPs, which is consistent with the previous discussion.

A bioelectrode that detected glucose was even prepared by integrating stable high-conductivity carbon into the 1D channels of ZnO nanowires with good electron transfer properties [11]. A ZnO nanowire array was coated with a thin layer of carbon by carbonization, without any observed NPs or aggregates. CV indicated that the electrode exhibited a pair of well-defined redox peaks, indicating the fast direct electrochemistry of GOx.

Detection of other analytes

Detecting uric acid in physiological fluids is important for diagnosing disorders associated with altered purine metabolism. Equations (3) and (4) describe the uricase catalyzing reaction:

$$\text{Uric acid} + O_2 \rightarrow \text{Allantoin} + CO_2 + H_2O_2, \quad (3)$$

$$H_2O_2 \rightarrow O_2 + 2H^+ + 2e^-. \quad (4)$$

A reagentless uric acid biosensor based on uricase-functionalized ZnO nanorods exhibited good thermal stability, anti-interference capability, and DET. It had an estimated K_M^{app} of 0.238 mM [77]. Introducing a stabilized lipid film between the ZnO and enzyme increased the activity duration of the uricase [78], and the positively charged lipid

film contributed to the sensitivity. Ali *et al.* [79] electrostatically immobilized uricase on ZnO nanoflakes, which were hydrothermally prepared at low temperature on Au-coated glass. The resulting uric acid biosensor exhibited a sensitivity of ~66 mV decade^{-1}, a logarithmic concentration range from 500 nM to 1.5 mM, and good selectivity against ascorbic acid, glucose and urea. N-doped ZnO thin films [80,81] and tetrapod-shaped ZnO nanostructures [82] have also been exploited as matrices in uric acid biosensors.

The catalytic reaction of lactate oxidase (LOD) in the detection of L-lactic acid is described by Equations (5) and (6):

$$\text{L-lactic acid} + O_2 \rightarrow \text{Pyruvate} + H_2O_2, \quad (5)$$

$$H_2O_2 \rightarrow O_2 + 2H^+ + 2e^-. \quad (6)$$

LOD was fixed on ZnO nanorods using a glutaraldehyde cross-linker. The resulting potentiometric electrochemical sensor exhibited a sensitivity of ~41 mV decade^{-1}, and a detection range from 0.1 μM to 1 mM [83]. A ZnO nanotetrapod network was used to adsorb LOD, because of its favorable 3D structure and electron transport properties [84]. ZnO NPs were decorated on MWCNTs (Fig. 2i), to provide a favorable microenvironment for LOD [49]. An electrochemiluminescence lactic acid biosensor based on the same structure was proposed, by combining analytical electrochemistry and luminescence spectroscopy [85]. A low detection limit (4 nM) was a result of the low background signal of the luminescence technique. The high electrocatalytic activity of the enzyme was retained by the nanohybrid.

The concentration of serum cholesterol is strongly correlated with many cardiovascular and cerebrovascular diseases. Accurately determining cholesterol levels in human blood is therefore important. The enzymatic reaction of cholesterol oxidase (ChOx) in cholesterol biosensors is described by Equations (7) and (8):

$$\text{Cholesterol} + O_2 \rightarrow \text{Cholest-4-en-3-one} + H_2O_2, \quad (7)$$

$$H_2O_2 \rightarrow O_2 + 2H^+ + 2e^-. \quad (8)$$

A ZnO nanostructured thin film was synthesized by vapor phase transport, and then loaded with ChOx. The resulting biosensor exhibited a of 1.08 mM, which indicated the high affinity of ChOx towards cholesterol [86]. Porous ZnO micro-tubes (Fig. 2j) were constructed using 3D assembled porous flakes. Giri *et al.* [50] exploited this structure in a cholesterol sensor, which exhibited a sensitivity of 54.5 μA mM^{-1} cm^{-2}. Ahmad *et al.* [87] grew an AR-controlled ZnO nanorod array on a Ag electrode, which was incorporated in a cholesterol biosensor, with a sensitivity of 74.10 μA mM^{-1} cm^{-2} and an upper detection limit of 16.0 mM. It exhibited anti-interference capability against electroactive species such as glucose, ascorbic acid, L-cysteine and uric acid. Wang *et al.* [88] reported Pt/Au hybrid-functionalized ZnO nanorods combined with a MWCNT layer, as a matrix for immobilized ChOx. Fig. 3 illustrates the preparation of this biosensor. The components interacted with each other, providing a favorable environment for the enzyme, and enhancing the analytical response of the biosensor. The detection limit was 0.03 μM. The enhancement was induced by the combination of the ZnO nanorods, nano Pt/Au and MWCNTs, which indicated the potential of nanocomposites in biosensing. ZnO thin films grown by pulsed laser deposition [89], and ZnO nanowalls with a lipid membrane [90], have also been used as platforms for ChOx immobilization.

ZnO nanorods were hydrothermally synthesized on Au wires, and used in the detection of H_2O_2 [91]. Poly(sodium-4-styrenesulfonate) (PSS) and horseradish peroxidase (HRP) layers were alternately immobilized on the ZnO surface. The multilayer structure largely retained the activity of the enzyme, with a K_M^{app} of 10.72 μM when three HRP layers were incorporated. A ZnO film containing electrodeposited Ag NPs was used in a H_2O_2 biosensor, which exhibited an ideal detection limit of 2 μM [92]. The threefold sensitivity enhancement (compared with the biosensor not containing ZnO) was attributed to the ZnO film facilitating the formation and distribution of the Ag NPs. HRP was effectively immobilized, based on the studies of the flower-like ZnO-Au NP-Nafion composite [93,94]. The biosensor demonstrated direct electrochemistry with enhanced electrocatalytic activity towards the reduction of H_2O_2. Other groups have immobilized HRP on flower-like ZnO/chitosan (Fig. 2k) [51], multiple forklike ZnO/chitosan (Fig. 2l) [52], and ZnO/poly[aniline-co-sodium *N*-(1-one-butyric acid)aniline] organic-inorganic composites [95].

Well-aligned single-crystal ZnO nanorods grown on Au-coated glass have been used for sensing penicillin. The nanorods were grown using a low temperature aqueous chemical method. The penicillinase enzyme was immobilized on the nanorods, via a *N*-5-azido-2-nitrobenzoyloxy-succinimide cross-linker [96]. Potentiometric investigation indicated that the sensor exhibited a linear response over a logarithmic concentration range from 100 μM to 100 mM,

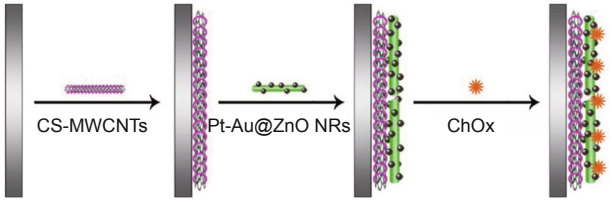

Figure 3 Preparation of the ChOx/Pt-Au@ZnO nanorod/chitosan-MWCNT biosensor [88] (Reproduced with permission from Elsevier).

and a sensitivity of ~121 mV decade^{-1}. The sensor exhibited negligible response to common interferents such as Na^+, K^+, *D*-glucose, *L*-glucose, ascorbic acid, and uric acid, so it is applicable in fermentation, medicine, and other related fields.

A positively charged ZnO sol-gel matrix [97], 3-aminopropyltriethoxysilane and tetraethoxysilane biofunctionalized ZnO nanorod microarrays [98], and CNT-ZnO-Nafion mesoporous composite films [99] have been shown to provide a favorable microenvironment for tyrosinase in tyrosine biosensors. Xanthine oxidase was covalently immobilized on a ZnO NPs/chitosan/MWCNTs/polyaniline composite, which was used to quantify xanthine in fish meat, providing potential application in quality control of fish industries [100].

Performance comparisons of ZnO nanostructures

Chemical vapor deposition (CVD) and hydrothermal processes are the most common approaches to controllably synthesize ZnO nanostructures. CVD typically involves exposing wafers to precursors, which react and/or decompose on the substrate surface to acquire the expected products. CVD can produce versatile ZnO nanostructures of high crystallinity, but is expensive and involves high energy consumption. Its low yield restricts its mass application. The simplicity and environmentally-friendliness of hydrothermal processes has promoted their popularity. Synthesis is carried out in aqueous media, with growth temperatures controlled at lower than the boiling point of water at a given pressure. A typical hydrothermal process involves preparing a ZnO seed layer from a zinc salt solution (e.g., zinc acetate hydrate nanocolloid) through the sol-gel route, and maintaining the immersed substrate at a certain temperature for several hours. ZnO nanostructures with precise morphologies can be prepared by adjusting the reaction conditions, such as the precursor concentration, growth time, temperature and pH. This method is suitable for growing large-scale high-quality crystals of controlled composition.

The performance of the biosensor primarily depends on the size, morphology, crystallinity, surface states and physical and chemical properties of the ZnO nanostructure. Therefore, an appropriate synthesis method and nanostructure modification are important for optimizing biosensor performance. Table 1 compares the performance of representative ZnO nanostructure-based electrochemical biosensors. Most have relatively low K_M^{app} values, indicating that the corresponding ZnO nanomaterials retain the enzyme activity. Biosensors possessing 3D spatial ZnO nanostructures usually exhibit wider linear ranges, because the large surface-to-volume ratio of the nanostructure allows more enzyme to be immobilized. Directly growing ZnO nanostructures on electrode substrates typically yields biosensors with faster response times. Transferring nanomaterials to electrode surfaces can give unsatisfactory contact between the ZnO and electrode, which significantly reduces electron transport and gives a slower response. Introducing metal or metal oxide NPs to the ZnO nanostructures can enhance the signal and sensitivity, because of the favorable electrocatalytic properties of the metal or metal oxide. Smaller NPs are more likely to reach active sites deeply embedded within the enzyme. The high conductivity of metal or metal oxide NPs can increase electron communication between the enzymes and the ZnO matrices, which makes it easier to realize DET during the electrochemical process. Introducing CNTs and graphene can give a moderate improvement in biosensor performance, because of their biocompatibility, high chemical and thermal stability, and high electron mobility.

BIOSENSORS BASED ON FIELD EFFECT TRANSDUCTION

Field effect transistors (FETs)

Converting a FET into a biosensor normally involves substituting the metal gate electrode with a bio-sensitive interface, which is brought into contact with the analyte solution. Enzyme FETs (ENFETs) have been developed in micron sizes, and exhibit fast responses, label-free analysis capability, ultrahigh sensitivity, real time analysis capability, batch processing capability, and the potential for chip integration [101,102]. ENFETs are based on ion sensitive FETs (ISFETs). ISFETs exploit the variation in conductance, resulting from a local potential generated by surface ions from a solution. ISFETs are used to measure pH and ionic concentrations (e.g., Na^+, K^+, Cl^-, NH_4^+, Ca^{2+}) [103]. The application of ISFETs as ENFET biosensors is realized when pH changes near the gate are mediated by specific enzymes, in the presence of their substance in a dose-dependent manner [104]. Small molecules including glucose [105], urea [106–108], acetylcholine [109], creatinine [107] and cholesterol [110] have been widely investigated using ENFETs. Most recent research has focused on silicon nanomaterials [111–113], Au nanowires [114] and CNTs [115–117], and a few studies have investigated metal oxide semiconductors. Silicon surfaces lack stability and are easily oxidized, which degrades device reliability. Au materials are costly, and challenges with chirality and defection exist for CNTs [118,119]. Thus, metal oxide semiconductors are promising candidates as FET gate electrode materials for biosensing applications.

Fig. 4 shows a single ZnO nanowire immobilized across Ti/Au layered electrodes [120]. The nanowire was prepared in a CVD furnace without catalyst, and the electrode was

Table 1 Representative ZnO nanostructure-based electrochemical biosensors

No	Schematic	Electrode	Analyte	Component 1	Component 2	ZnO Fabrication Process	Sensitivity ($\mu A\ cm^{-2}\ mM^{-1}$)	Linear range (mM)	LOD (μM)	K_M (mM)	Response time (s)	Ref.
1	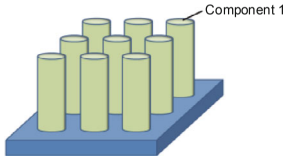	Au	Glucose	ZnO nanorod array	/	Hydro-thermal	23.1	0.01–3.45	10	2.9	< 5	[30]
2	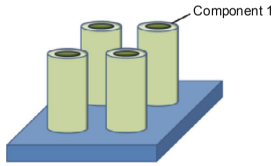	ITO	Glucose	ZnO nanotube array	/	Electro-chemical/ chemical	30.85	0.01–4.2	10	2.59	< 6	[37]
3	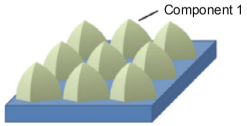	GCE	Glucose	Tetragonal pyramid-shaped ZnO	/	Hydro-thermal	/	0.05–8.2	10	/	/	[12]
4	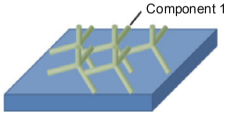	Au	Glucose	Tetrapod-like ZnO	/	CVD	25.3	0.005–6.5	4	5.05	6	[26]
5	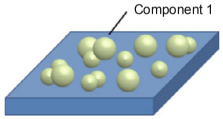	Pt	Glucose	ZnO NPs	/	Solution-thermal	/	/	5.6	/	/	[29]
6	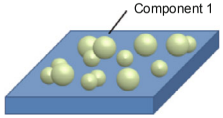	Au	Glucose	ZnO nanofi-bers	/	Electro-spinning	70.2	0.25–19	1	2.19	< 4	[28]
7	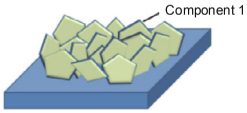	Glass capillary	Glucose	ZnO nano-flakes	/	Hydro-thermal	–65.2 mV decade^{-1}	0.0005–10	0.5	/	< 4	[40]

(*To be continued on the next page*)

(*Continued*)

No	Schematic	Electrode	Analyte	Component 1	Component 2	ZnO Fabrication Process	Sensitivity ($\mu A\ cm^{-2}\ mM^{-1}$)	Linear range (mM)	LOD (μM)	K_M (mM)	Response time (s)	Ref.
8	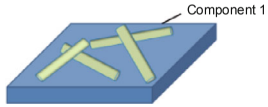	GCE	Uric acid	ZnO nanorods	/	/	t	0.005–1.0	2	0.238	/	[77]
9	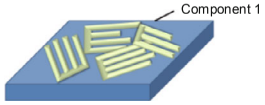	GCE	H_2O_2	Fork-like ZnO	/	Annealing	201.12 $\mu A\ mM^{-1}$	0.05–0.7	0.3	0.292	3	[52]
10	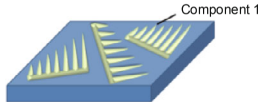	Au	Glucose	Comb-like ZnO	/	CVD	15.33	0.02–4.5	20	2.19	< 10	[9]
11	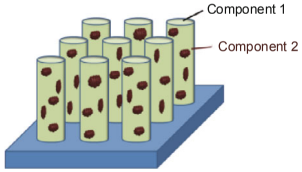	Ti	Glucose	ZnO nanorod array	Carbon	Hydro-thermal	35.3	0.01−1.6	1	1.54	4	[11]
12	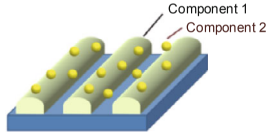	ITO	Glucose	Periodic 1D ZnO array	Au NPs	Lithogra-phy	/	/	/	/	/	[61]
13	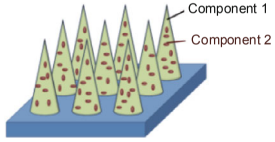	ITO	Glucose	ZnO array matrix	Cu	Hydro-thermal	97 nA mM^{-1}	1−15	40	/	< 6	[48]
14	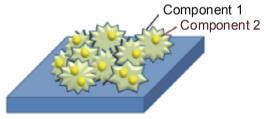	GCE	H_2O_2	Flower-like ZnO	Au NPs	Hydro-thermal	/	0.015−1.1	9	1.76	/	[93]
15	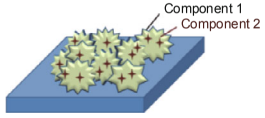	PET/ Ti/Au	Glucose	ZnO nanoclus-ter matrix	Co	Magnetron sput-tering	13.3	0.2–4	20	21	8	[63]

(*To be continued on the next page*)

(*Continued*)

No	Schematic	Electrode	Analyte	Component 1	Component 2	ZnO Fabrication Process	Sensitivity ($\mu A\ cm^{-2}\ mM^{-1}$)	Linear range (mM)	LOD (μM)	K_M (mM)	Response time (s)	Ref.
16	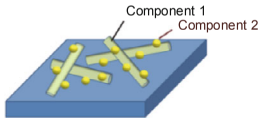	GCE	Glucose	ZnO nanorods	Au NPs	Hydro-thermal	1492	0.1–33.0	0.01	0.41	< 5	[58]
17	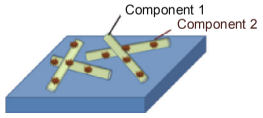	Pt	Glucose	ZnO nanorods	NiO	Hydro-thermal	61.78	0.5–8.0	2.5	7.4	< 5	[62]
18	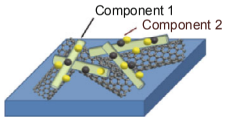	GCE	Cholest-erol	ZnO nanorods	Pt-Au	Hydro-thermal	26.8 $\mu A\ mM^{-1}$	0.0001–0.7593	0.03	1.84	< 6	[88]
19	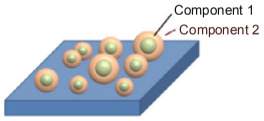	ITO	Glucose	ZnO NPs	Chitosan-graft-PVA	/	> 0.04 V μM^{-1}	0.002–1.2	0.2	/	3	[54]
20	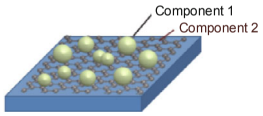	ITO	Glucose	ZnO NPs	Graphene	Hydro-thermal	/	/	/	/	/	[13]
21	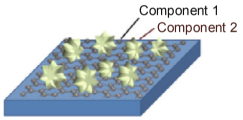	GCE	Glucose	ZnO micro-flowers	Reduced graphene oxide	Electro-deposition	18.97 $\mu A\ mM^{-1}$	0.02–6.24	20	/	/	[75]
22	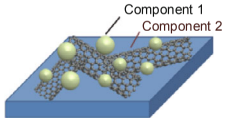	PGE (pyrolytic graphite)	Glucose	ZnO NPs	MWCNTs	CVD	50.2	0.1–16.0	0.25	8.9	6	[73]
23	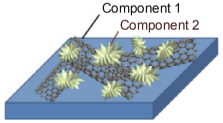	GCE	Glucose	ZnO micro-sponge	MWCNTs	Electro-deposition	4.18	0.2–27.2	20	/	3–5	[74]

prepared by electron-beam lithography. The electrodes were passivated with polymethyl methacrylate (PMMA), to decrease current leakage and the effect of metal-nanowire contact. The characteristics of the fabricated FET were investigated. The drain current *vs*. drain voltage characteristics were obtained as a function of different gate voltages, and the on/off ratio and transconductance were ~4.6×10^6 and ~8.2 nS, respectively. The nanowire was then functionalized with uricase via cross-linking, and applied in the detection of uric acid. The response time of the sensor was in the order of milliseconds, and the detection limit was 1 pM for a 14.7 nS increase in conductance. Thus, the undoped ZnO nanowire with n-type properties could be used as a FET biosensor. Patterned ZnO nanorods hydrothermally synthesized on selected areas were integrated as glucose FET sensors [121]. GOx modified with both covalent and electrostatic bonding has been characterized, and indicated a large amount of GOx was immobilized on the ZnO nanorods. To achieve a real-time response towards cholesterol with high sensitivity, ChOx was immobilized on the active layer of vertically aligned ZnO nanorods, between the source and drain electrodes [110]. The solution-gated FET sensor exhibited a detection limit of ~0.05 μM, and low interference from electroactive species.

Extended gate FETs (EGFET) are alternatives to traditional FETs. EGFETs are robust, easily fabricated, and low cost. The extended gate allows the FET to be isolated from the chemical environment, in case of hindering the measurement process. The extended gate arrangement facilitates detection in small sample volumes, illustrating the potential of nanostructures coupled with standard electronic components for biosensing. ZnO nanowires were grown on 250-μm-diameter Ag wire at low temperature, functionalized with GOx [122], and then used as the extended gate of a commercial metal-oxide-semiconductor field effect transistor (MOSFET) in a glucose biosensor. The electrochemical response on the gate surface induced a voltage change, which modulated the current through the MOSFET. High quality ZnO thin films and nanorods were prepared by a vapor cooling condensation system, and were used as the gate electrode of an EGFET glucose biosensor [123]. A photoelectrochemical method was adopted to improve sensing performance, by passivating dangling bonds and surface states of ZnO nanorod sidewalls. The Fermi level pining effect was therefore diminished, indicating that the sensitivity was improved by the passivated ZnO nanorods.

High electron mobility transistors (HEMTs)

HEMTs with high 2D electron gas (2DEG) mobility and saturation velocity have been applied in sensing platforms [124–128]. Slight ambient changes affect the surface charges of the HEMT during detection, which are transduced into a change in 2DEG concentration. Thus, the drain current also changes.

AlGaN/GaN HEMT with a high electron sheet carrier concentration channel was used to fabricate a glucose biosensor. The channel was induced by piezoelectric and spontaneous polarization between the AlGaN and GaN layers [125]. To immobilize GOx, the ZnO nanorod array was selectively grown on the gate area, through low temperature hydrothermal decomposition. This also increased the total sensing area (Fig. 5). The glucose concentration was measured from the drain current with the change in charge of the ZnO nanorods, and the detection signal was amplified through the HEMT. The drain-source current response time was < 5 s, and the detection limit was 0.5 nM. The same HEMT structure was also functionalized with LOD, and used in a lactic acid biosensor [126]. The

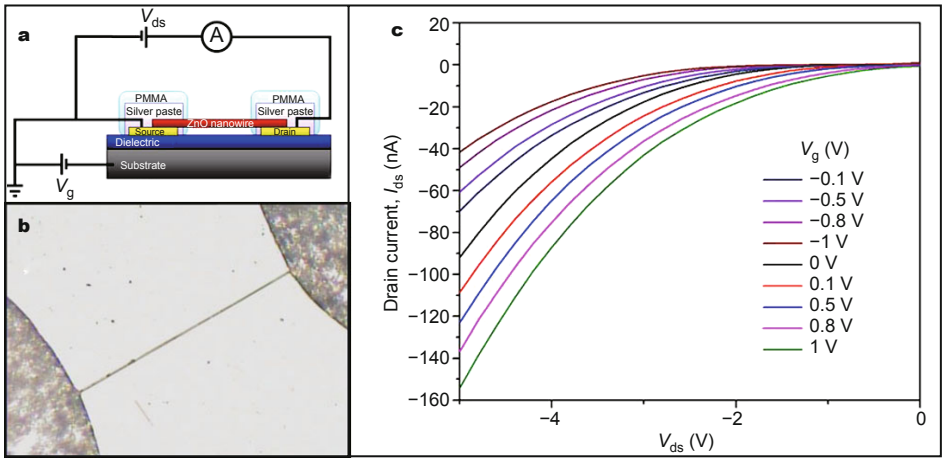

Figure 4 (a) Schematic and (b) optical image of a single ZnO nanowire FET biosensor. (c) I_{ds}–V_{ds} measurements under varying V_g, at V_{ds} = −1 V (Reproduced with permission from Ref. [120], Copyright 2013, Elsevier).

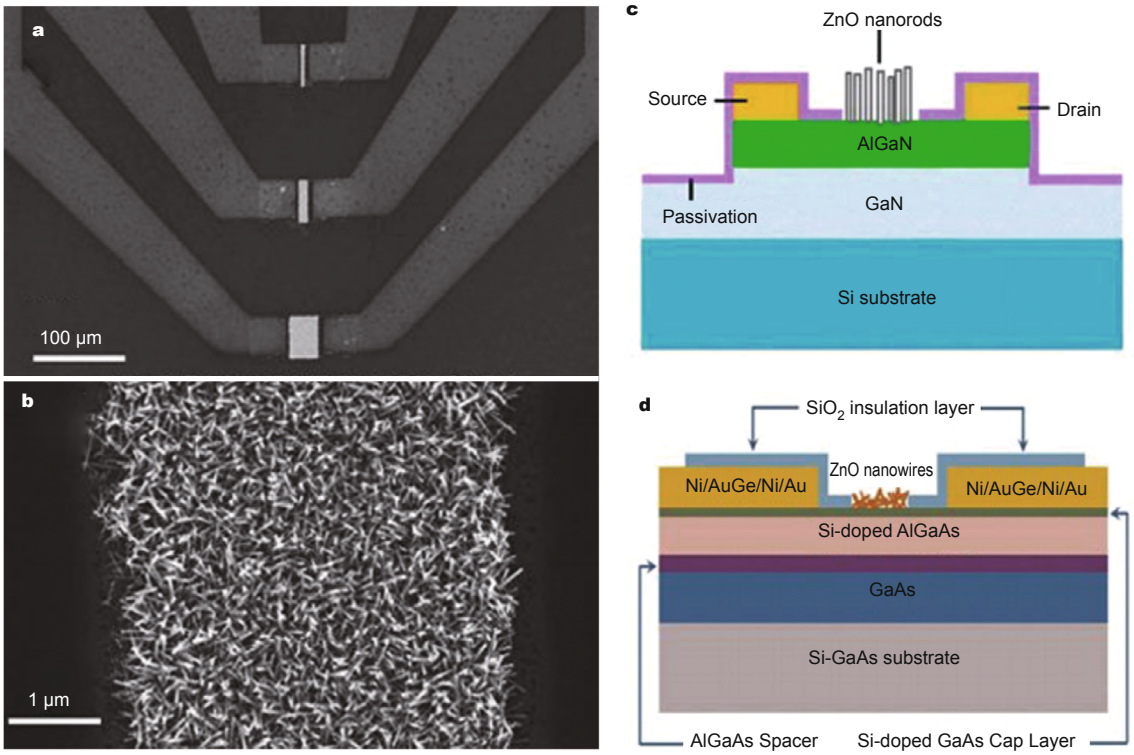

Figure 5 (a) SEM image of an AlGaN/GaN HEMT sensor, with three gates of different sizes. (b) SEM image of the ZnO nanorod array in the gate region. (c) Schematic cross sectional view of the ZnO nanorod-gated AlGaN/GaN HEMT ((a–c) Reproduced with permission from Ref. [126], Copyright 2008, AIP Publishing LLC). (d) Schematic cross sectional view of the ZnO nanowire-gated AlGaAs/GaAs HEMT (Reproduced with permission from Ref. [127], Copyright 2012, Royal Society of Chemistry).

limit of detection was 167 nM, because of the amplification effect by the HEMT. Ma *et al.* [127] used a AlGaAs/GaAs HEMT with ZnO nanowires immobilized at the gate region, for lactic acid detection. The electrons in the AlGaAs/GaAs HEMT could be excited more easily than those in the AlGaN/GaN HEMT, because the energy gap of GaAs (1.42 eV) is narrower than that of GaN (3.44 eV). The addition of a Si-doped GaAs cap layer onto the Si-doped AlGaAs layer enhanced the chemical stability of the gate, and improved the transport of the carrier in the cap layer. A detection limit of 0.03 nM was achieved. The low energy consumption, miniaturization, prompt detection, and low cost of HEMTs make them attractive for further research and development, particularly in medical and bioassay applications. Combining HEMT technology and nanotechnology with biosensing may promote the design and fabrication of electronic biosensing devices.

CHALLENGES AND OUTLOOK

ZnO nanostructures can serve as bridges between biological receptors and transistors. Their advantages include their size scale, specific surface area, electrical conductivity and biocompatibility, which are apparent from their application in electrochemical sensors and field effect transistors. However, many challenges remain in the design of highly efficient, miniaturized, wireless, implantable diagnostic devices.

ZnO nanostructures suitable for versatile application should be synthesized, through simultaneously controlling their dimensions, morphologies, and properties. Advanced techniques like electron beam evaporation, molecular beam epitaxy, sputtering, nanoimprint lithography, and phase-shift optical lithography have been used for this purpose. Innovative ZnO-based nanocomposites, such as inorganic-organic and metal-semiconductor hybrids, should be developed, because of their interesting structures and properties resulting from the combination of each component. For example, ZnO/Au hybrids deserve additional attention, since Au nanomaterials are already used in clinical applications. The Schottky barrier that forms at the interface between ZnO and Au can significantly affect electron transport, and may be exploited to facilitate electron transfer between redox enzymes and transducers, thus improving biosensor performance. Nanostructures grown directly on electrodes provide more favorable electron exchange between the electrode and the nanomaterial matrix, than

those transferred to electrode surfaces. Thus, nanostructures synthesized *in situ* on electrodes are preferred for biosensor construction. Perhaps the most important focus should be on the sensitivity of biosensor performance with respect to ZnO nanomaterial morphology. The synthesis of new ZnO nanostructures should be guided by the potential for an improved device.

Many biosensors containing ZnO or ZnO-based nanocomposites exhibit DET, without the presence of mediators [9,11–13,54,57,60,61,77,78]. Investigating DET is important for understanding the kinetics and thermodynamics of biological redox processes, and for fabricating next-generation biosensors. Enzyme-active centers are typically deeply embedded within the enzyme structure, making it difficult for electrons to transfer to conventional electrodes [129]. However, zero-dimensional (e.g., NPs) and 1D nanomaterials (e.g., nanowires) are of comparable size to the enzyme's redox center, so DET is more easily realized using these matrices. Electrodes modified with CNTs, graphene, and Au NPs have been used to facilitate DET of enzymes. Hybridizing these nanomaterials with nano-ZnO will likely enhance DET, and improve biosensor performance.

The integration of "ideal" ZnO nanostructures must also be considered. It is important to immobilize nanomaterials at specific locations in FET-based devices. Unfortunately, nanomaterials are frequently randomly spread on electrode surfaces. Techniques for manipulating, locating and immobilizing nanomaterials should therefore be encouraged. These include dielectrophoresis for nanowire alignment, nano-manipulation or scanning probe microscopy for controlling or locating nanomaterials, and focused ion beam for depositing metal layers and thus immobilizing nanostructures.

The fluorescence of ZnO nanocrystals has been exploited using photoluminescence (PL) spectroscopy to realize glucose detection [130]. ZnO NPs were coated with mercaptoundecanoic acid (MUA) via the polyol method. MUA served as a template for synthesizing spherical NPs, and as an organic linker to form bioconjugates with GOx. The PL intensity of the ZnO-MUA-GOx bioconjugates decreased with increased glucose concentration. This was because of collisional quenching by H_2O_2 produced during glucose oxidation. The degree of PL quenching was proportional to the amount of H_2O_2, which in turn was proportional to the glucose concentration. While the upper detection limit was 33.3 mM, the lower detection limit was only 0.33 mM, which is far below the performance of electrochemical transduction or FET-based biosensors. Such optical-based methods remain an area for further exploration. Besides, wurtzite and zinc blend semiconductors such as ZnO usually exhibit piezoelectric properties, which can be exploited to tune the electron transport properties [131–136]. Yu *et al.* [137] reported a ZnO nanowire sensor with a metal-semiconductor-metal structure. The sensor was enhanced by the piezotronic effect, and detected the immunoglobulin G-targeted protein. A piezopotential was produced along the *c*-axis of the ZnO nanowire by applying compressive strain. This tuned the effective height of the Schottky barrier at contact, and influenced the output signal of the device. Exploiting the piezotronic effect of ZnO nanowires increased the device resolution by tens of times, and also improved the detection limit and sensitivity. The piezotronic effect could theoretically be introduced into ZnO-based enzyme biosensors to enhance their performance.

ZnO-enzyme systems offer many advantages for detecting biomolecules, and their continued development will benefit their clinical application. ZnO nanostructure-based enzyme biosensors are easily and cheaply produced, and their performance can satisfy clinical requirements. Commercial developments in ZnO-enzyme-based biosensors are likely in the coming years. The future of biosensing will undoubtedly involve integration and miniaturization. The remote monitoring of glucose has been realized through a functionalized ZnO nanowire array-based biosensor, integrated with a commercial mobile phone [138]. Data can be transferred through the Global System for Mobiles Communications (GSM) network, and then used for centralized monitoring. Such applications can reduce health care costs, and allow caregivers to examine and possibly treat patients from a distance.

CONCLUSIONS

ZnO nanostructures as enzyme matrices show significant potential for use in biosensors. The high performance of ZnO nanostructure-based enzyme biosensors can be attributed to the following points. First, diverse ZnO morphologies prepared from controlled syntheses possess large specific surface area, so they can be used to fabricate devices with different structures. Second, ZnO nanostructures with high IEPs promote the electrostatic adsorption of enzymes. Their biocompatibility also provides a favorable micro-environment for retaining enzyme activity. Third, high crystallinity of ZnO nanostructures can provide direct electron conduction tunnels between the enzyme active sites and electrode surface, without requiring a mediator. Opportunities and inspirations arising from ZnO nanostructures, nanotechnology and enzyme biosensors will advance the biosensor industry.

Received 6 November 2014; accepted 6 January 2015; published online 23 January 2015

1 Turner APF. Biosensors: sense and sensibility. Chem Soc Rev, 2013, 42: 3184–3196

2 Dzyadevych SV, Arkhypova VN, Soldatkin AP, *et al*. Amperometric enzyme biosensors: past, present and future. IRBM, 2008, 29: 171–180
3 Zhao Z, Lei W, Zhang X, *et al*. ZnO-based amperometric enzyme biosensors. Sensors, 2010, 10: 1216–1231
4 Ariga K, Ji Q, Mori T, *et al*. Enzyme nanoarchitectonics: organization and device application. Chem Soc Rev, 2013, 42: 6322–6345
5 Ravindra NM, Prodan C, Fnu S, *et al*. Advances in the manufacturing, types, and applications of biosensors. JOM, 2007, 59: 37–43
6 Zhou J, Xu NS, Wang ZL. Dissolving behavior and stability of ZnO wires in biofluids: a study on biodegradability and biocompatibility of ZnO nanostructures. Adv Mater, 2006, 18: 2432–2435
7 Li Z, Yang R, Yu M, *et al*. Cellular level biocompatibility and biosafety of ZnO nanowires. J Phys Chem C, 2008, 112: 20114–20117
8 Topoglidis E, Palomares E, Astuti Y, *et al*. Immobilization and electrochemistry of negatively charged proteins on modified nanocrystalline metal oxide electrodes. Electroanalysis, 2005, 17: 1035–1041
9 Wang J, Sun XW, Wei A, *et al*. Zinc oxide nanocomb biosensor for glucose detection. Appl Phys Lett, 2006, 88: 233106
10 Zhao Y, Yan X, Kang Z, *et al*. Highly sensitive uric acid biosensor based on individual zinc oxide micro/nanowires. Microchim Acta, 2013, 180: 759–766
11 Liu J, Guo C, Li CM, *et al*. Carbon-decorated ZnO nanowire array: a novel platform for direct electrochemistry of enzymes and biosensing applications. Electrochem Commun, 2009, 11: 202–205
12 Dai Z, Shao G, Hong J, *et al*. Immobilization and direct electrochemistry of glucose oxidase on a tetragonal pyramid-shaped porous ZnO nanostructure for a glucose biosensor. Biosens Bioelectron, 2009, 24: 1286–1291
13 Kavitha T, Gopalan AI, Lee KP, Park SY. Glucose sensing, photocatalytic and antibacterial properties of graphene–ZnO nanoparticle hybrids. Carbon, 2012, 50: 2994–3000
14 Jafari M, Khodadadi AA, Mortazavi Y, Ghorchian H. Deposition of ZnO nanopraticles on MWCNTs for glucose oxidase direct electrochemistry. IMCS 2012—The 14th International Meeting on Chemical Sensors, 2012, 687–689
15 Weiss RG, Chacko V, Glickson JD, Gerstenblith G. Comparative ^{13}C and ^{31}P NMR assessment of altered metabolism during graded reductions in coronary flow in intact rat hearts. Proc Natl Acad Sci USA, 1989, 86: 6426–6430
16 Hellman B, Idahl LÅ, Lernmark Å, Täljedal IB. The pancreatic β-cell recognition of insulin secretagogues: does cyclic AMP mediate the effect of glucose? Proc Natl Acad Sci USA, 1974, 71: 3405–3409
17 Zawalich WS, Matschinsky FM. Sequential analysis of the releasing and fuel function of glucose in isolated perifused pancreatic islets. Endocrinology, 1977, 100: 1–8
18 Sweet I, Li G, Najafi H, *et al*. Effect of a glucokinase inhibitor on energy production and insulin release in pancreatic islets. Am J Physiol Endoc M, 1996, 271: 606–625
19 Guillam MT, Dupraz P, Thorens B. Glucose uptake, utilization, and signaling in GLUT2-null islets. Diabetes, 2000, 49: 1485–1491
20 Passonneau JV, Lowry OH. Enzymatic Analysis: A Practical Guide. Totowa: Humana Press, 1993
21 Moley KH, Chi MMY, Mueckler MM. Maternal hyperglycemia alters glucose transport and utilization in mouse preimplantation embryos. Am J Physiol Endoc M, 1998, 275: 38–47
22 Ronkainen NJ, Halsall HB, Heineman WR. Electrochemical biosensors. Chem Soc Rev, 2010, 39: 1747–1763
23 Liu CC. Electrochemical based biosensors. Biosensors, 2012, 2: 269–272
24 Arya SK, Saha S, Ramirez-Vick JE, *et al*. Recent advances in ZnO nanostructures and thin films for biosensor applications: review. Anal Chim Acta, 2012, 737: 1–21
25 Topoglidis E, Cass AE, O'Regan B, Durrant JR. Immobilisation and bioelectrochemistry of proteins on nanoporous TiO_2 and ZnO films. J Electroanal Chem, 2001, 517: 20–27
26 Lei Y, Yan X, Luo N, *et al*. ZnO nanotetrapod network as the adsorption layer for the improvement of glucose detection via multiterminal electron-exchange. Colloids Surf A, 2010, 361: 169–173
27 Aydogdu G, Zeybek DK, Pekyardimci Ş, Kiliç E. A novel amperometric biosensor based on ZnO nanoparticles-modified carbon paste electrode for determination of glucose in human serum. Artif Cells Nanomed Biotechnol, 2013, 41: 332–338
28 Ahmad M, Pan C, Luo Z, Zhu J. A single ZnO nanofiber-based highly sensitive amperometric glucose biosensor. J Phys Chem C, 2010, 114: 9308–9313
29 Ren X, Chen D, Meng X, *et al*. Zinc oxide nanoparticles/glucose oxidase photoelectrochemical system for the fabrication of biosensor. J Colloid Interface Sci, 2009, 334: 183–187
30 Wei A, Sun XW, Wang J, *et al*. Enzymatic glucose biosensor based on ZnO nanorod array grown by hydrothermal decomposition. Appl Phys Lett, 2006, 89: 123902
31 Liu X, Hu Q, Wu Q, *et al*. Aligned ZnO nanorods: a useful film to fabricate amperometric glucose biosensor. Colloids Surf B, 2009, 74: 154–158
32 Ahmad R, Tripathy N, Kim JH, Hahn YB. Highly selective wide linear-range detecting glucose biosensors based on aspect-ratio controlled ZnO nanorods directly grown on electrodes. Sens Actuators B, 2012, 174: 195–201
33 Kim JY, Jo SY, Sun GJ, *et al*. Tailoring the surface area of ZnO nanorods for improved performance in glucose sensors. Sens Actuators B, 2014, 192: 216–220
34 Pradhan D, Niroui F, Leung K. High-performance, flexible enzymatic glucose biosensor based on ZnO nanowires supported on a gold-coated polyester substrate. ACS Appl Mater Interfaces, 2010, 2: 2409–2412
35 Lei Y, Yan X, Zhao J, *et al*. Improved glucose electrochemical biosensor by appropriate immobilization of nano-ZnO. Colloids Surf B, 2011, 82: 168–172
36 Jung J, Lim S. ZnO nanowire-based glucose biosensors with different coupling agents. Appl Surf Sci, 2013, 265: 24–29
37 Yang K, She GW, Wang H, *et al*. ZnO nanotube arrays as biosensors for glucose. J Phys Chem C, 2009, 113: 20169–20172
38 Kong T, Chen Y, Ye Y, *et al*. An amperometric glucose biosensor based on the immobilization of glucose oxidase on the ZnO nanotubes. Sens Actuators B, 2009, 138: 344–350
39 Ali SMU, Kashif M, Ibupoto ZH, *et al*. Functionalised zinc oxide nanotube arrays as electrochemical sensors for the selective determination of glucose. Micro Nano Lett, 2011, 6: 609–613
40 Fulati A, Ali SMU, Asif MH, *et al*. An intracellular glucose biosensor based on nanoflake ZnO. Sens Actuators B, 2010, 150: 673–680
41 Asif MH, Ali SMU, Nur O, *et al*. Functionalised ZnO-nanorod-based selective electrochemical sensor for intracellular glucose. Biosens Bioelectron, 2010, 25: 2205–2211
42 Fatemi H, Khodadadi AA, Firooz AA, Mortazavi Y. Apple–biomorphic synthesis of porous ZnO nanostructures for glucose direct electrochemical biosensor. Curr Appl Phys, 2012, 12: 1033–1038
43 Zhao M, Li Z, Han Z, *et al*. Synthesis of mesoporous multiwall ZnO nanotubes by replicating silk and application for enzymatic biosensor. Biosens Bioelectron, 2013, 49: 318–322
44 Belcher AM, Wu X, Christensen R, *et al*. Control of crystal phase switching and orientation by soluble mollusc-shell proteins. Nature, 1996, 381: 56–58
45 Cha JN, Stucky GD, Morse DE, Deming TJ. Biomimetic synthesis of ordered silica structures mediated by block copolypeptides. Nature, 2000, 403: 289–292
46 Nuraje N, Su K, Haboosheh A, *et al*. Room temperature synthesis of ferroelectric barium titanate nanoparticles using peptide nanorings as templates. Adv Mater, 2006, 18: 807–811
47 Zhao M, Huang J, Zhou Y, *et al*. A single mesoporous ZnO/Chi-

tosan hybrid nanostructure for a novel free nanoprobe type biosensor. Biosens Bioelectron, 2013, 43: 226–230
48 Yang C, Xu C, Wang X. ZnO/Cu nanocomposite: a platform for direct electrochemistry of enzymes and biosensing applications. Langmuir, 2012, 28: 4580–4585
49 Wang Y, Yu L, Wang J, *et al*. A novel L-lactate sensor based on enzyme electrode modified with ZnO nanoparticles and multiwall carbon nanotubes. J Electroanal Chem, 2011, 661: 8–12
50 Giri AK, Sinhamahapatra A, Prakash S, *et al*. Porous ZnO microtubes with excellent cholesterol sensing and catalytic properties. J Mater Chem A, 2013, 1: 814–822
51 Liu YL, Yang YH, Yang HF, *et al*. Nanosized flower-like ZnO synthesized by a simple hydrothermal method and applied as matrix for horseradish peroxidase immobilization for electro-biosensing. J Inorg Biochem, 2005, 99: 2046–2053
52 Yang Z, Zong X, Ye Z, *et al*. The application of complex multiple forklike ZnO nanostructures to rapid and ultrahigh sensitive hydrogen peroxide biosensors. Biomaterials, 2010, 31: 7534–7541
53 Liu H, Zuo Z, Guo Y, *et al*. Supramolecular interactions at the inorganic-organic interface in hybrid nanomaterials. Angew Chem Int Ed, 2010, 122: 2705–2707
54 Shukla S, Deshpande SR, Shukla SK, Tiwari A. Fabrication of a tunable glucose biosensor based on zinc oxide/chitosan-graft-poly(vinyl alcohol) core-shell nanocomposite. Talanta, 2012, 99: 283–287
55 Yeom SH, Kang BH, Kim KJ, Kang SW. Nanostructures in biosensor—a review. Front Biosci Landmark Ed, 2010, 16: 997–1023
56 Lee SH, Sung JH, Park TH. Nanomaterial-based biosensor as an emerging tool for biomedical applications. Ann Biomed Eng, 2012, 40: 1384–1397
57 Zhang L, Wang Y, Wang J, *et al*. rhEPO/EPO discrimination with ultrasensitive electrochemical biosensor based on sandwich-type nano-Au/ZnO sol-gel/nano-Au signal amplification. Biosens Bioelectron, 2013, 50: 217–223
58 Wei Y, Li Y, Liu X, *et al*. ZnO nanorods/Au hybrid nanocomposites for glucose biosensor. Biosens Bioelectron, 2010, 26: 275–278
59 Bhattacharya A, Jain C, Rao VP, Banerjee S. Gold coated ZnO nanorod biosensor for glucose detection. AIP Conf Proc, 2012, 1447: 295–296
60 Zhang J, Wang C, Chen S, *et al*. Amperometric glucose biosensor based on glucose oxidase-lectin biospecific interaction. Enzyme Microb Technol, 2013, 52: 134–140
61 Huh P, Kim M, Kim SC. Glucose sensor using periodic nanostructured hybrid 1D Au/ZnO arrays. Mater Sci Eng C, 2012, 32: 1288–1292
62 Chu X, Zhu X, Dong Y, *et al*. An amperometric glucose biosensor based on the immobilization of glucose oxidase on the platinum electrode modified with NiO doped ZnO nanorods. J Electroanal Chem, 2012, 676: 20–26
63 Zhao Z, Chen X, Tay B, *et al*. A novel amperometric biosensor based on ZnO: Co nanoclusters for biosensing glucose. Biosens Bioelectron, 2007, 23: 135–139
64 Yang W, Ratinac KR, Ringer SP, *et al*. Carbon nanomaterials in biosensors: should you use nanotubes or graphene? Angew Chem Int Ed, 2010, 49: 2114–2138
65 Liu Y, Dong X, Chen P. Biological and chemical sensors based on graphene materials. Chem Soc Rev, 2012, 41: 2283–2307
66 Hahn Y-B, Ahmad R, Tripathy N. Chemical and biological sensors based on metal oxide nanostructures. Chem Commun, 2012, 48: 10369–10385
67 Chen W, Cai S, Ren QQ, *et al*. Recent advances in electrochemical sensing for hydrogen peroxide: a review. Analyst, 2012, 137: 49–58
68 Walcarius A, Minteer SD, Wang J, *et al*. Nanomaterials for bio-functionalized electrodes: recent trends. J Mater Chem B. 2013, 1: 4878–4908
69 Wang G, Tan X, Zhou Q, *et al*. Synthesis of highly dispersed zinc oxide nanoparticles on carboxylic graphene for development a sensitive acetylcholinesterase biosensor. Sens Actuators B, 2014, 190: 730–736
70 Yue HY, Huang S, Chang J, *et al*. ZnO Nanowire arrays on 3D-hierarchical graphene foam: biomarker detection of Parkinson's disease. ACS Nano, 2014, 8: 1639–1646
71 Tak M, Gupta V, Tomar M. Zinc oxide–multiwalled carbon nanotubes hybrid nanocomposite based urea biosensor. J Mater Chem B, 2013, 1: 6392–6401
72 Hu F, Chen S, Wang C, *et al*. ZnO nanoparticle and multiwalled carbon nanotubes for glucose oxidase direct electron transfer and electrocatalytic activity investigation. J Mol Catal B Enzym, 2011, 72: 298–304
73 Wang YT, Yu L, Zhu ZQ, *et al*. Improved enzyme immobilization for enhanced bioelectrocatalytic activity of glucose sensor. Sens Actuators B, 2009, 136: 332–337
74 Palanisamy S, Cheemalapati S, Chen SM. Enzymatic glucose biosensor based on multiwalled carbon nanotubes-zinc oxide composite. Int J Electrochem Sci, 2012, 7: 8394–8407
75 Palanisamy S, Vilian A, Chen SM. Direct electrochemistry of glucose oxidase at reduced graphene oxide/zinc oxide composite modified electrode for glucose sensor. Int J Electrochem Sci, 2012, 7: 2153–2163
76 Dey RS, Raj CR. A hybrid functional nanoscaffold based on reduced graphene oxide–ZnO for the development of an amperometric biosensing platform. RSC Adv, 2013, 3: 25858–25864
77 Zhang F, Wang X, Ai S, *et al*. Immobilization of uricase on ZnO nanorods for a reagentless uric acid biosensor. Anal Chim Acta, 2004, 519: 155–160
78 Tzamtzis N, Psychoyios VN, Nikoleli GP, *et al*. Flow potentiometric injection analysis of uric acid using lipid stabilized films with incorporated uricase on ZnO nanowires. Electroanalysis, 2012, 24: 1719–1725
79 Ali SMU, Ibupoto ZH, Kashif M, *et al*. A potentiometric indirect uric acid sensor based on ZnO nanoflakes and immobilized uricase. Sensors, 2012, 12: 2787–2797
80 Jindal K, Tomar M, Gupta V. Nitrogen-doped zinc oxide thin films biosensor for determination of uric acid. Analyst, 2013, 138: 4353–4362
81 Jindal K, Tomar M, Gupta V. Inducing electrocatalytic functionality in ZnO thin film by N doping to realize a third generation uric acid biosensor. Biosens Bioelectron, 2014, 55: 57–65
82 Lei Y, Liu X, Yan X, *et al*. Multicenter uric acid biosensor based on tetrapod-shaped ZnO nanostructures. J Nanosci Nanotechno, 2012, 12: 513–518
83 Ibupoto ZH, Shah SMU, Khun K, Willander M. Electrochemical L-lactic acid sensor based on immobilized ZnO nanorods with lactate oxidase. Sensors, 2012, 12: 2456–2466
84 Lei Y, Luo N, Yan X, *et al*. A highly sensitive electrochemical biosensor based on zinc oxide nanotetrapods for L-lactic acid detection. Nanoscale, 2012, 4: 3438–3443
85 Haghighi B, Bozorgzadeh S. Fabrication of a highly sensitive electrochemiluminescence lactate biosensor using ZnO nanoparticles decorated multiwalled carbon nanotubes. Talanta, 2011, 85: 2189–2193
86 Batra N, Tomar M, Gupta V. Realization of an efficient cholesterol biosensor using ZnO nanostructured thin film. Analyst, 2012, 137: 5854–5859
87 Ahmad R, Tripathy N, Hahn YB. Wide linear-range detecting high sensitivity cholesterol biosensors based on aspect-ratio controlled ZnO nanorods grown on silver electrodes. Sens Actuators B, 2012, 169: 382–386
88 Wang C, Tan X, Chen S, *et al*. Highly-sensitive cholesterol biosensor based on platinum-gold hybrid functionalized ZnO nanorods. Talanta, 2012, 94: 263–270

89 Batra N, Tomar M, Gupta V. Efficient detection of cholesterol using ZnO thin film based matrix. J Exp Nanosci, 2013, 8: 280–287
90 Psychoyios VN, Nikoleli GP, Tzamtzis N, *et al*. Potentiometric cholesterol biosensor based on ZnO nanowalls and stabilized polymerized lipid film. Electroanalysis, 2013, 25: 367–372
91 Gu B, Xu C, Zhu G, *et al*. Layer by layer immobilized horseradish peroxidase on zinc oxide nanorods for biosensing. J Phys Chem B, 2009, 113: 6553–6557
92 Wang Q, Zheng J. Electrodeposition of silver nanoparticles on a zinc oxide film: improvement of amperometric sensing sensitivity and stability for hydrogen peroxide determination. Microchim Acta, 2010, 169: 361–365
93 Xiang C, Zou Y, Sun L, Xu F. Direct electrochemistry and enhanced electrocatalysis of horseradish peroxidase based on flowerlike ZnO-gold nanoparticle-Nafion nanocomposite. Sens Actuators B, 2009, 136: 158–162
94 Zhang Y, Zhang Y, Wang H, *et al*. An enzyme immobilization platform for biosensor designs of direct electrochemistry using flower-like ZnO crystals and nano-sized gold particles. J Electroanal Chem, 2009, 627: 9–14
95 Chen HC, Hua MY, Liu YC, *et al*. Preparation of water-dispersible poly[aniline-co-sodium *N*-(1-one-butyric acid) aniline]–zinc oxide nanocomposite for utilization in an electrochemical sensor. J Mater Chem, 2012, 22: 13252–13259
96 Ibupoto ZH, Ali SMU, Khun K, *et al*. ZnO nanorods based enzymatic biosensor for selective determination of penicillin. Biosensors, 2011, 1: 153–163
97 Liu Z, Liu Y, Yang H, *et al*. A mediator-free tyrosinase biosensor based on ZnO sol-gel matrix. Electroanalysis, 2005, 17: 1065–1070
98 Zhao J, Wu D, Zhi J. A novel tyrosinase biosensor based on biofunctional ZnO nanorod microarrays on the nanocrystalline diamond electrode for detection of phenolic compounds. Bioelectrochemistry, 2009, 75: 44–49
99 Lee JM, Xu GR, Kim BK, *et al*. Amperometric tyrosinase biosensor based on carbon nanotube-doped sol-gel-derived zinc oxide-Nafion composite films. Electroanalysis, 2011, 23: 962–970
100 Devi R, Yadav S, Pundir C. Amperometric determination of xanthine in fish meat by zinc oxide nanoparticle/chitosan/multiwalled carbon nanotube/polyaniline composite film bound xanthine oxidase. Analyst, 2012, 137: 754–759
101 Pohanka M, Skládal P. Electrochemical biosensors—principles and applications. J Appl Biomed, 2008, 6: 57–64
102 Torsi L, Magliulo M, Manoli K, Palazzo G. Organic field-effect transistor sensors: a tutorial review. Chem Soc Rev, 2013, 42: 8612–8628
103 Miao YQ, Guan JG, Chen JR. Ion sensitive field effect transducer-based biosensors. Biotechnol Adv, 2003, 21: 527–534
104 Vijayalakshmi A, Tarunashree Y, Baruwati B, *et al*. Enzyme field effect transistor (ENFET) for estimation of triglycerides using magnetic nanoparticles. Biosens Bioelectron, 2008, 23: 1708–1714
105 Soldatkin A, El'Skaya A, Shul'ga A, *et al*. Glucose-sensitive field-effect transistor with additional Nafion membrane: reduction of influence of buffer capacity on the sensor response and extension of its dynamic range. Anal Chim Acta, 1993, 283: 695–701
106 Jaffrezic-Renault N, Wan K, Senillou A, *et al*. Development of new polymeric membranes for ENFETs for biomedical and environmental applications. Analysis, 1999, 27: 578–586
107 Hamlaoui M, Reybier K, Marrakchi M, *et al*. Development of a urea biosensor based on a polymeric membrane including zeolite. Anal Chim Acta, 2002, 466: 39–45
108 Premanode B, Toumazou C. A novel, low power biosensor for real time monitoring of creatinine and urea in peritoneal dialysis. Sens Actuators B, 2007, 120: 732–735
109 Hai A, Ben-Haim D, Korbakov N, *et al*. Acetylcholinesterase–ISFET based system for the detection of acetylcholine and acetylcholinesterase inhibitors. Biosens Bioelectron, 2006, 22: 605–612
110 Ahmad R, Tripathy N, Hahn YB. High-performance cholesterol sensor based on the solution-gated field effect transistor fabricated with ZnO nanorods. Biosens Bioelectron, 2013, 45: 281–286
111 Cui Y, Zhong Z, Wang D, *et al*. High performance silicon nanowire field effect transistors. Nano Lett, 2003, 3: 149–152
112 Duan X, Li Y, Rajan NK, *et al*. Quantification of the affinities and kinetics of protein interactions using silicon nanowire biosensors. Nat Nanotechnol, 2012, 7: 401–407
113 Patolsky F, Zheng G, Lieber CM. Fabrication of silicon nanowire devices for ultrasensitive, label-free, real-time detection of biological and chemical species. Nat Protoc, 2006, 1: 1711–1724
114 Lapierre-Devlin MA, Asher CL, Taft BJ, *et al*. Amplified electrocatalysis at DNA-modified nanowires. Nano Lett, 2005, 5: 1051–1055
115 Maehashi K, Katsura T, Kerman K, *et al*. Label-free protein biosensor based on aptamer-modified carbon nanotube field-effect transistors. Anal Chem, 2007, 79: 782–787
116 So HM, Won K, Kim YH, *et al*. Single-walled carbon nanotube biosensors using aptamers as molecular recognition elements. J Am Chem Soc, 2005, 127: 11906–11907
117 Kim JP, Lee BY, Hong S, Sim SJ. Ultrasensitive carbon nanotube-based biosensors using antibody-binding fragments. Anal Biochem, 2008, 381: 193–198
118 Fujisawa K, Komiyama K, Muramatsu H, *et al*. Chirality-dependent transport in double-walled carbon nanotube assemblies: the role of inner tubes. ACS Nano, 2011, 5: 7547–7554
119 Gayathri V, Geetha R. Carbon nanotube as NEMS sensor-effect of chirality and stone-wales defect intend. J Phys Conf Ser, 2006, 34: 824–828
120 Liu X, Lin P, Yan X, *et al*. Enzyme-coated single ZnO nanowire FET biosensor for detection of uric acid. Sens Actuators B, 2013, 176: 22–27
121 Ogata K, Dobashi H, Koike K, *et al*. Patterned growth of ZnO nanorods and enzyme immobilization toward the fabrication of glucose sensors. Physica E, 2010, 42: 2880–2883
122 Ali SM, Nur O, Willander M, Danielsson B. Glucose detection with a commercial MOSFET using a ZnO nanowires extended gate. IEEE Transact Nanotechnol, 2009, 8: 678–683
123 Lee CT, Chiu YS, Ho SC, Lee YJ. Investigation of a photoelectrochemical passivated ZnO-based glucose biosensor. Sensors, 2011, 11: 4648–4655
124 Kang B, Wang HT, Ren F, *et al*. AlGaN/GaN HEMT and ZnO nanorod based sensors for chemical and bio-applications. ECS Trans, 2008, 13: 53–63
125 Kang B, Wang H, Ren F, *et al*. Enzymatic glucose detection using ZnO nanorods on the gate region of AlGaN/GaN high electron mobility transistors. Appl Phys Lett, 2007, 91: 252103
126 Chu B, Kang B, Ren F, *et al*. Enzyme-based lactic acid detection using AlGaN/GaN high electron mobility transistors with ZnO nanorods grown on the gate region. Appl Phys Lett, 2008, 93: 042114
127 Ma S, Liao Q, Liu H, *et al*. An excellent enzymatic lactic acid biosensor with ZnO nanowires-gated AlGaAs/GaAs high electron mobility transistor. Nanoscale, 2012, 4: 6415–6418
128 Zhang X, Zhang Y, Liao Q, *et al*. Reduced graphene oxide-functionalized high electron mobility transistors for novel recognition pattern label-free DNA sensors. Small, 2013, 9: 4045–4050
129 Li N, Xu JZ, Yao H, *et al*. The direct electron transfer of myoglobin based on the electron tunneling in proteins. J Phys Chem B, 2006, 110: 11561–11565
130 Kim KE, Kim TG, Sung YM. Enzyme-conjugated ZnO nanocrystals for collisional quenching-based glucose sensing. CrystEngComm, 2012, 14: 2859–2865
131 Wang ZL. Piezopotential gated nanowire devices: piezotronics and piezo-phototronics. Nano Today, 2010, 5: 540–552
132 Zhang Y, Yan X, Yang Y, *et al*. Scanning probe study on the piezotronic effect in ZnO nanomaterials and nanodevices. Adv Ma-

ter, 2012, 24: 4647–4655
133 Yang Y, Qi J, Liao Q, *et al*. High-performance piezoelectric gate diode of a single polar-surface dominated ZnO nanobelt. Nanotechnology, 2009, 20: 125201–125205
134 Dai Y, Zhang Y, Wang Z. The octa-twin tetraleg ZnO nanostructures. Solid State Commun, 2003, 126: 629–633
135 Dai Y, Zhang Y, Bai Y, *et al*. Bicrystalline zinc oxide nanowires. Chem Phys Lett, 2003, 375: 96–101
136 Zhang Y, Yang Y, Gu Y, *et al*. Performance and service behavior in 1-D nanostructured energy conversion devices. Nano Energy, doi: 10.1016/j.nanoen.2014.12.039
137 Yu R, Pan C, Wang ZL. High performance of ZnO nanowire protein sensors enhanced by the piezotronic effect. Energy Environ Sci, 2013, 6: 494–499
138 Ali SMU, Aijazi T, Axelsson K, *et al*. Wireless remote monitoring of glucose using a functionalized ZnO nanowire arrays based sensor. Sensors, 2011, 11: 8485–8496

Acknowledgements This work was supported by the National Basic Research Program of China (2013CB932600), the Major Project of International Cooperation and Exchanges (2012DFA50990), the Program of Introducing Talents of Discipline to Universities, the National Natural Science Foundation of China (51232001, 51172022 and 51372023), the Research Fund of Co-construction Program from Beijing Municipal Commission of Education, the Fundamental Research Funds for the Central Universities, and the Program for Changjiang Scholars and Innovative Research Team in University.

Author contributions Zhang Y and Kang Z wrote the manuscript. Yan X and Liao Q investigated and analyzed published literature. All authors discussed and provided feedback on the manuscripts structure, arguments and conclusions.

Conflict of interest The authors declare that they have no conflicts of interest.

Yue Zhang is vice-president of the University of Science & Technology Beijing. He received his PhD in Materials Physics from the University of Science & Technology Beijing in 1993. He has been awarded the financial support for outstanding young scientist foundation of China and selected as the chief scientist of Major National Scientific Research Projects. His research focuses on nanoenergy device and integration, information-sensing nanodevice and nanosystem, as well as nanomaterial and nanodevice service behavior. He has published more than 300 papers in peer reviewed scientific journals and 8 monographs, and held 25 patents in his research area. His publication has been cited more than 3000 times by peers.

中文摘要 自从Liland C. Clark Jr. 于1962年首次发明生物传感器以来, 生物传感技术得到了突飞猛进的发展. 目前, 氧化锌纳米材料被视为极有前景的生物传感器构建材料之一, 其具有多样化的纳米结构、高电子迁移率、化学稳定性、电化学活性、高等电点、生物相容性、压电特性等一系列出众的优异性能. 本综述从电化学器件以及场效应器件两个角度介绍了氧化锌纳米材料在酶基生物传感器领域的应用. 通过不同的合成工艺而获得的氧化锌纳米结构被用于酶分子的装载与固定, 并同时为酶提供一个良好的微环境, 从而有效提升了生物传感性能. 本文综述了氧化锌纳米材料合成工艺的最新进展, 针对不同的氧化锌纳米结构对传感器的性能进行了对比, 并总结了氧化锌纳米材料在生物传感器构建中的主要优势, 以及未来的发展前景和挑战.